ELSEVIER

AIRSAR Studies of Woody Shrub Density in Semiarid Rangeland: Jornada del Muerto, New Mexico

H. Brad Musick, Gerald S. Schaber,† and Carol S. Breed†*

This study evaluates the use of polarimetric Airborne Synthetic Aperture Radar (AIRSAR) data to assess woody shrub density in a semiarid site where the vegetation consists primarily of varied mixtures of herbaceous vegetation and shrubs. AIRSAR data and field observations of vegetation cover and growth form-composition were obtained for 59 sites in the Jornada del Muerto plain in southern New Mexico. Radar signature measures examined were C-, L- and P-band backscattering coefficients (σ^0) for HH, HV and VV polarizations, ratios of σ^0HH and σ^0HV to σ^0VV, and the HH–VV polarization phase difference and correlation coefficient. The most effective measure for estimation of shrub density was L-band σ^0HV, which distinguished among shrub density classes with no misclassification. Sensitivity of this measure to small amounts of shrub cover was indicated by successful separation of sites with <1% shrub cover from sites with 1–5% cover. Separability of shrub density classes was generally least for C-band signature measures. A distinctive radar signature was exhibited by dense stands of Yucca elata*, a semitreelike plant with uniformly thick (≈10 cm diameter) fibrous stems. Yucca sites were distinguished from others by their high P-band σ^0HV relative to L-band σ^0HV. The results are largely explained by the greater sensitivity of longer wavelengths to larger canopy structural elements. L-band σ^0HV and other measures responsive to canopy volume scattering were more strongly related to shrub than to herbaceous plant cover because woody shrub canopies have numerous stems of the intermediate size to which L-band is most sensitive, whereas stems of this size are mostly lacking in herbaceous canopies. The uniform-diameter stems of yucca have larger dimensions to which P-band is more sensitive than L-band. ©Elsevier Science Inc., 1998*

INTRODUCTION

Replacement of semidesert grassland by woody shrubland is a widespread form of desertification. This change in physiognomy and species composition tends to sharply reduce the productivity of the land for grazing by domestic livestock, increase soil erosion and reduce soil fertility, and greatly alter many other aspects of ecosystem structure and functioning (Schlesinger et al., 1990).

Remote sensing methods are needed to assess and monitor shrubland encroachment. Sensitive methods capable of detecting woody shrubs at low density would provide useful information for management and prediction because an initially low shrub density often tends to increase even after cessation of the disturbance (e.g., overgrazing, drought, or fire suppression) responsible for triggering the initial stages of the invasion (Grover and Musick, 1990). In contrast to other forms of desertification, biomass does not consistently decrease with a shift from grassland to shrubland. Therefore, remotely sensed estimates of green vegetation amount do not provide a consistently reliable means of detecting shrub invasion.

Radar responses to aridland vegetation have been studied less than those of forest and cropland vegetation. Observations and modeling of radar backscatter from forests consistently indicate a sensitivity to size and orientation of canopy structural elements (Dobson et al., 1992; Ferrazzoli et al., 1992; Le Toan et al., 1992; Moghaddam and Saatchi, 1995; Kasischke et al., 1995; Ferrazzoli and Guerriero, 1995). Applicability of these results to aridland vegetation cannot be assumed, because such vegetation is

* University of New Mexico, Albuquerque
† U.S. Geological Survey, Flagstaff

Address correspondence to Brad Musick, 625 Florida SE, Albuquerque, NM 87108. E-mail: BRAD_MUSICK@nmenv.state.nm.us
Received 22 September 1997; revised 17 April 1998.

REMOTE SENS. ENVIRON. 66:29–40 (1998)

655 Avenue of the Americas, New York, NY 10010

0034-4257/98/$19.00
PII S0034-4257(98)00033-9

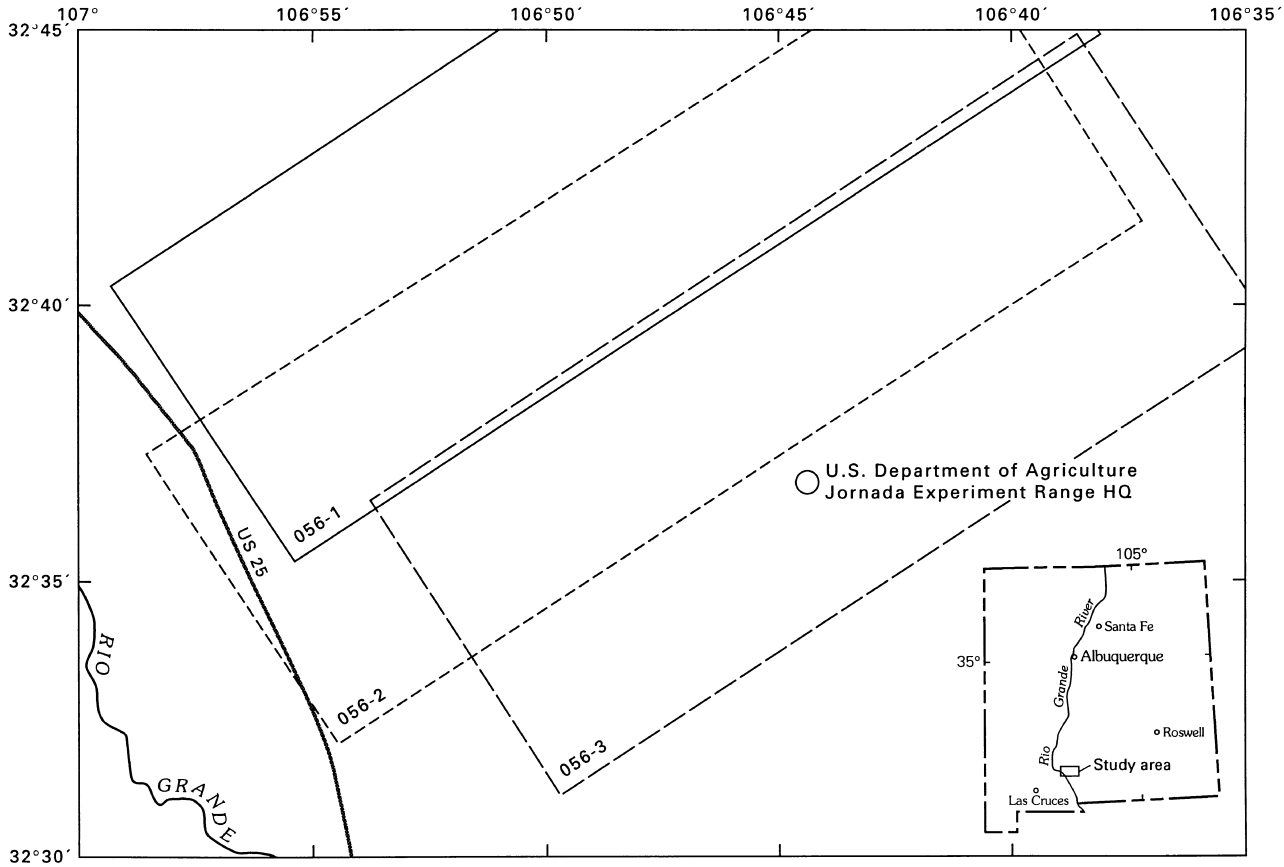

Figure 1. Index map of study site showing AIRSAR passes acquired 1 August 1990. Coverage (solid and dashed rectangles) and mission-pass numbers (e.g., 056-2) of SAR images described here are indicated. Small inset map (lower right) shows location of the study site in New Mexico along with major cities and the Rio Grande; distance across large map is 39.2 km.

much lower in biomass than forests, and coverage of the ground surface by vegetation is discontinuous.

Most observations of radar response of aridland vegetation have been made in studies primarily concerned with geologic mapping (Evans et al., 1986; 1988) or estimation of surface roughness. In studies of aeolian terrain in arid regions, radar has proven useful in distinguishing stable, vegetated areas from bare areas of active sand movement (Blom and Elachi, 1981; Greeley et al., 1989; Greeley and Blumberg, 1995). However, Lancaster et al. (1992) attributed the greater radar-brightness of the vegetated areas to small-scale roughness resulting from accumulation of wind-blown sediment in mounds around the bases of the plants, rather than to backscatter from the plants themselves.

The objective of this study was to determine if the potential sensitivity of active microwave remote sensing to vegetation structure could be used to assess the degree of shrub invasion of grassland. Polarimetric Airborne Synthetic Aperture Radar (AIRSAR) data were acquired from NASA/JPL for a semiarid site containing varied mixtures of shrubs and herbaceous vegetation and compared with ground observations of vegetation type and other land-surface characteristics. Responses of backscattering power intensity to shrub density were examined.

METHODS

Study Site

The study site is in the southern Jornada del Muerto plain in south-central New Mexico (Fig. 1). The area includes the study site of the Jornada Long-Term Ecological Research (LTER) Project. Also included in the area are private and federally managed grazing land and two long-established range management research facilities, the USDA/ARS Jornada Experimental Range and the New Mexico State University College Ranch, as well as a geometeorological station operated by the Climate Program of the U.S. Geological Survey (Breed and Reheis, in press).

The terrain covered by the data sets has low relief. A wide variety of soils are represented, with surface soil texture ranging from sandy and loamy on uplands to silty and clayey in swales and depressions. Gravelly soils are also common on alluvial fans at the eastern margin of the plain, but they were not sampled in this study.

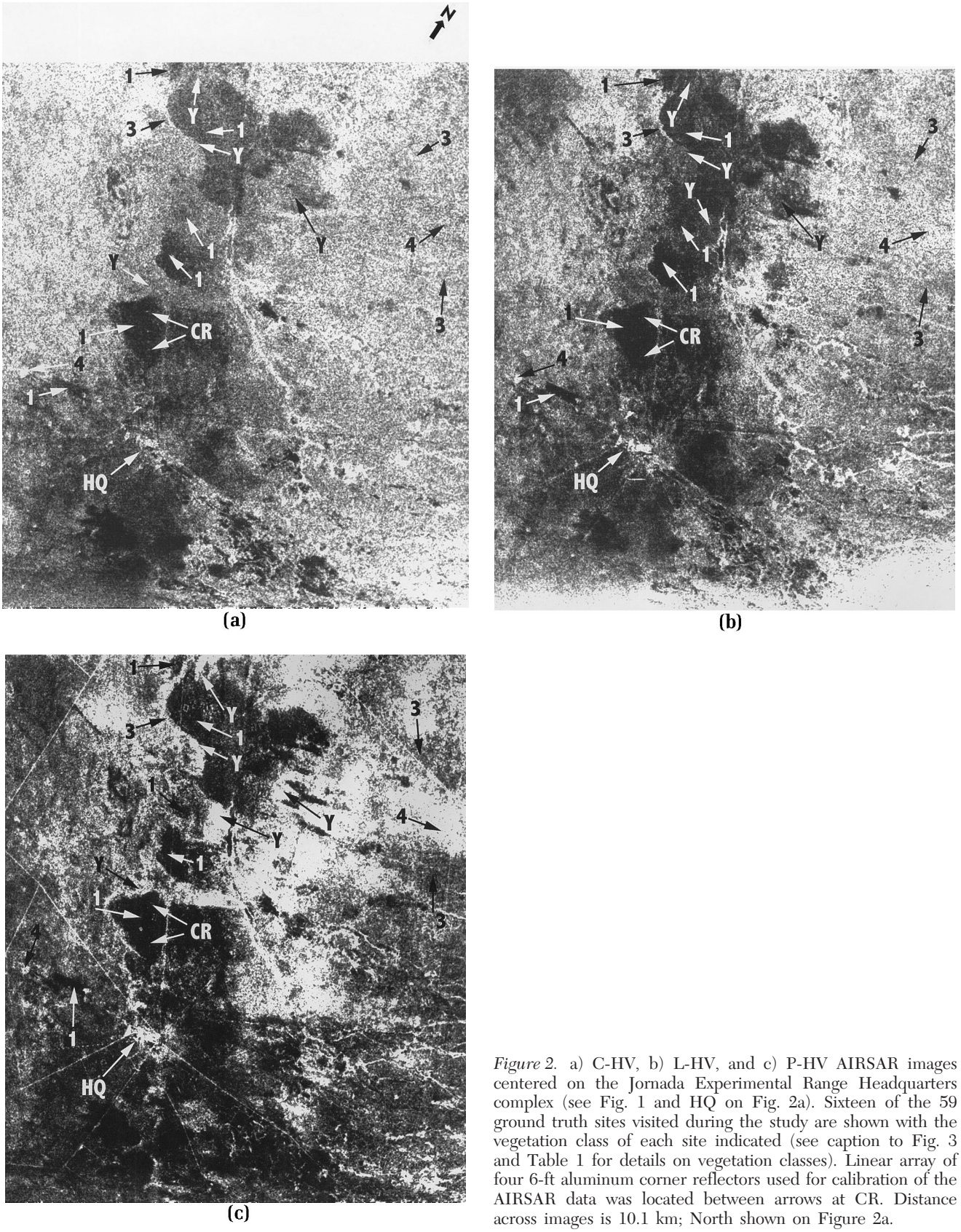

Figure 2. a) C-HV, b) L-HV, and c) P-HV AIRSAR images centered on the Jornada Experimental Range Headquarters complex (see Fig. 1 and HQ on Fig. 2a). Sixteen of the 59 ground truth sites visited during the study are shown with the vegetation class of each site indicated (see caption to Fig. 3 and Table 1 for details on vegetation classes). Linear array of four 6-ft aluminum corner reflectors used for calibration of the AIRSAR data was located between arrows at CR. Distance across images is 10.1 km; North shown on Figure 2a.

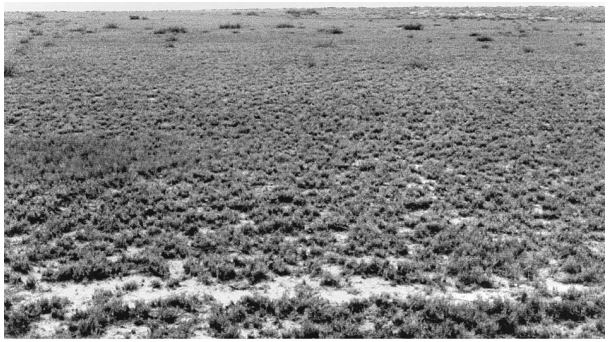

(a)

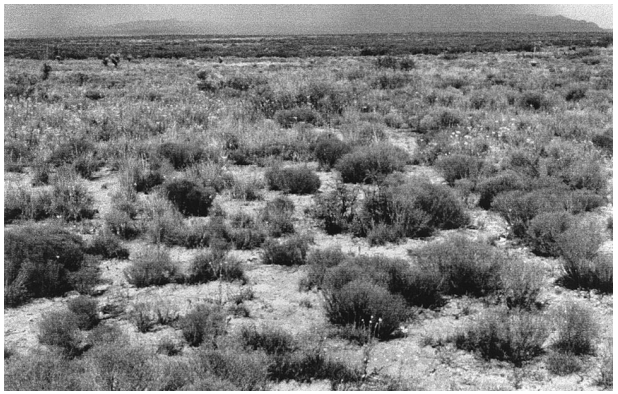

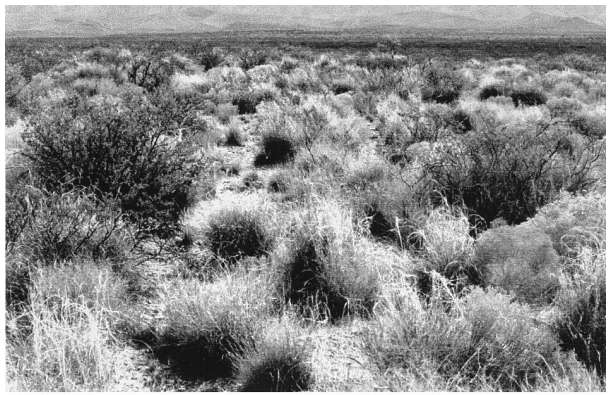

(b)

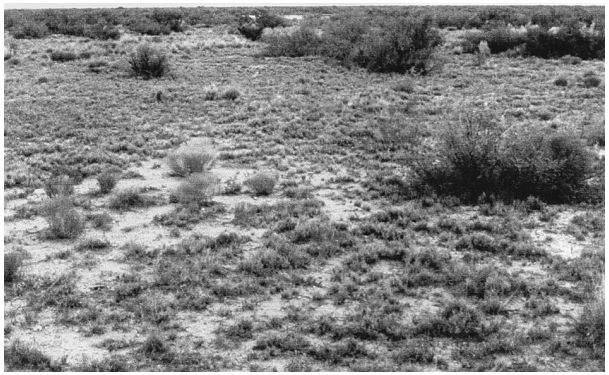

(c)

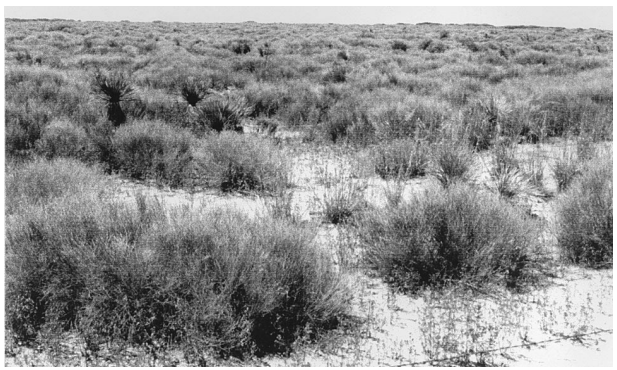

Figure 3. Ground photographs showing three examples each of the five vegetation classes: a–d) woody shrub density Classes 1–4, respectively (see Table 1); e) Class Y, abundant *Yucca elata*. Note wide range of herbaceous biomass, especially in Class 1(a).

Table 1. Woody Shrub Cover Classes

Class	*Woody Shrub Cover (%)*
1	<1
2	1–5
3	5–25
4	>25

Grassland occupied >90% of the area in the mid-1800s, but shrubland encroachment reduced grassland area to less than 25% over the next century (Buffington and Herbel, 1965). In recent years, this trend has been partially reversed only by herbicide treatment or mechanical removal of shrubs from some parts of the area. Mesquite (*Prosopis juliflora*) is the most abundant woody shrub; others include *Acacia* spp., tarbush (*Flourensia cernua*), and creosotebush (*Larrea tridentata*). Another common invader of grasslands is broom snakeweed (*Gutierrezia sarothrae*), a perennial subshrub. This species is woody only at the base of the stems (Pieper and McDaniel, 1989) and is thus not considered a woody shrub.

Management practices have created some sharply defined boundaries between shrubland and herbaceous vegetation. For example, marked contrasts in shrub density are sometimes found between adjacent pastures that differ in their grazing history. Distinct shrub-free patches surrounded by shrubland have been created by herbicide treatment and the mechanical removal of shrubs.

Multifrequency, fully polarimetric, SAR data were acquired at C-band (6-cm wavelength), L-band (24 cm), and P-band (68 cm) on 1 August 1990, by the NASA/JPL Airborne Synthetic Aperture Radar (AIRSAR) platform (DC-8-72). Examples of these data are shown in Figure 2. Two of the three parallel flightlines barely overlapped and covered an area approximately 30 km along-track by 22 km across-track (Fig. 1). The area covered by the third flightline was centered over the other two lines. Sites covered by the third flightline could thus be viewed at contrasting incidence angles.

Rainfall during the month before the overflight was above normal, and both herbaceous plants and shrubs were in leaf. During the week before the overflight, most rain gauges on the Jornada Experimental Range recorded from 6 mm to over 12 mm of rain, and precipitation fell over much of the area on the day of the overflight (R. P. Gibbens, personal communication). Volumetric soil moisture content was found to be spatially variable and to range from 1.4 g cm^{-3} to 1.7 g cm^{-3} in the seven soil samples collected from 5 cm to 40 cm below the surface on the day of the AIRSAR overflight. Signal penetration into the soil is therefore assumed to have been minimal, even at P-band. The moderately high soil moisture content in the blow sand and underlying soil is also reflected by the 2.6 dB higher average P-VV backscatter values for the Jornada site compared to the P-HH values (VV images not shown here). The 68-cm wavelength P-band SAR signals penetrate significantly deeper into sand and sandy soil than do the C-band and L-band signals. The P-band signals, therefore, are most sensitive to moisture in a volumetric sense, as well as to the associated high dielectric salts present in the upper meter or so of the surface. SAR data acquired in VV polarization are especially sensitive to the presence of soil moisture.

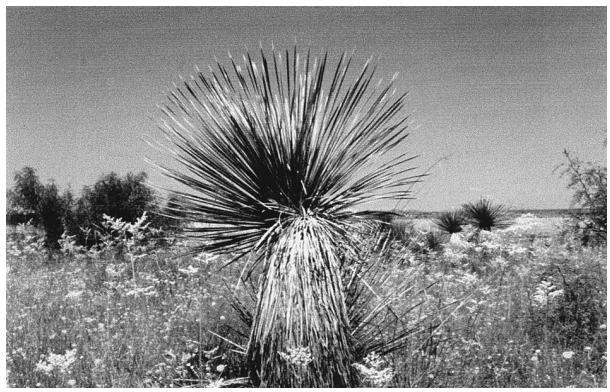

Figure 4. Close-up photograph of the monocotyledonous species *Yucca elata* showing details of the species' distinct morphology. This includes an unbranched to sparsely branched fibrous stem with high water content and the conical to nearly spherical spray of fibrous leaves (see Fig. 3e, Class Y).

Ground Truth

Field observations were made 17–27 August 1993. Fifty-nine sites were visited in the field and delineated as polygons on black-and-white prints of the images. In many cases, accurate delineation of sites on the images and in the field was facilitated by choosing sites bounded on one or more sides by fences. Fences constructed using only steel fenceposts were very bright features on the P-HV imagery (Fig. 2c). Sites selected to be relatively homogeneous in vegetation and radar signature were photographed, and visual estimates of vegetation composition and soil properties were recorded.

The sites were classified primarily according to percentage of ground area covered by woody shrub canopies (Fig. 3, Table 1). The major woody shrub species on most sites was mesquite, but some sites were dominated by other shrub species. Sites with a high density of soaptree yucca (*Yucca elata*) were assigned to a separate class (Y) after preliminary analyses indicated that these sites had a distinctive radar signature. This monocotyledonous species also exhibits a distinctive morphology (Figs. 3 and 4); the fibrous stems are unbranched to sparsely branched, 10–15 cm in diameter, 0.5–3.0 m tall, and high in water content. The apex of each stem bears a conical to nearly spherical spray of fibrous leaves 0.6–1.2 cm wide and 25–75 cm long (Martin and Hutchins, 1980). Counts made in one small (300 m^2) plot in a mod-

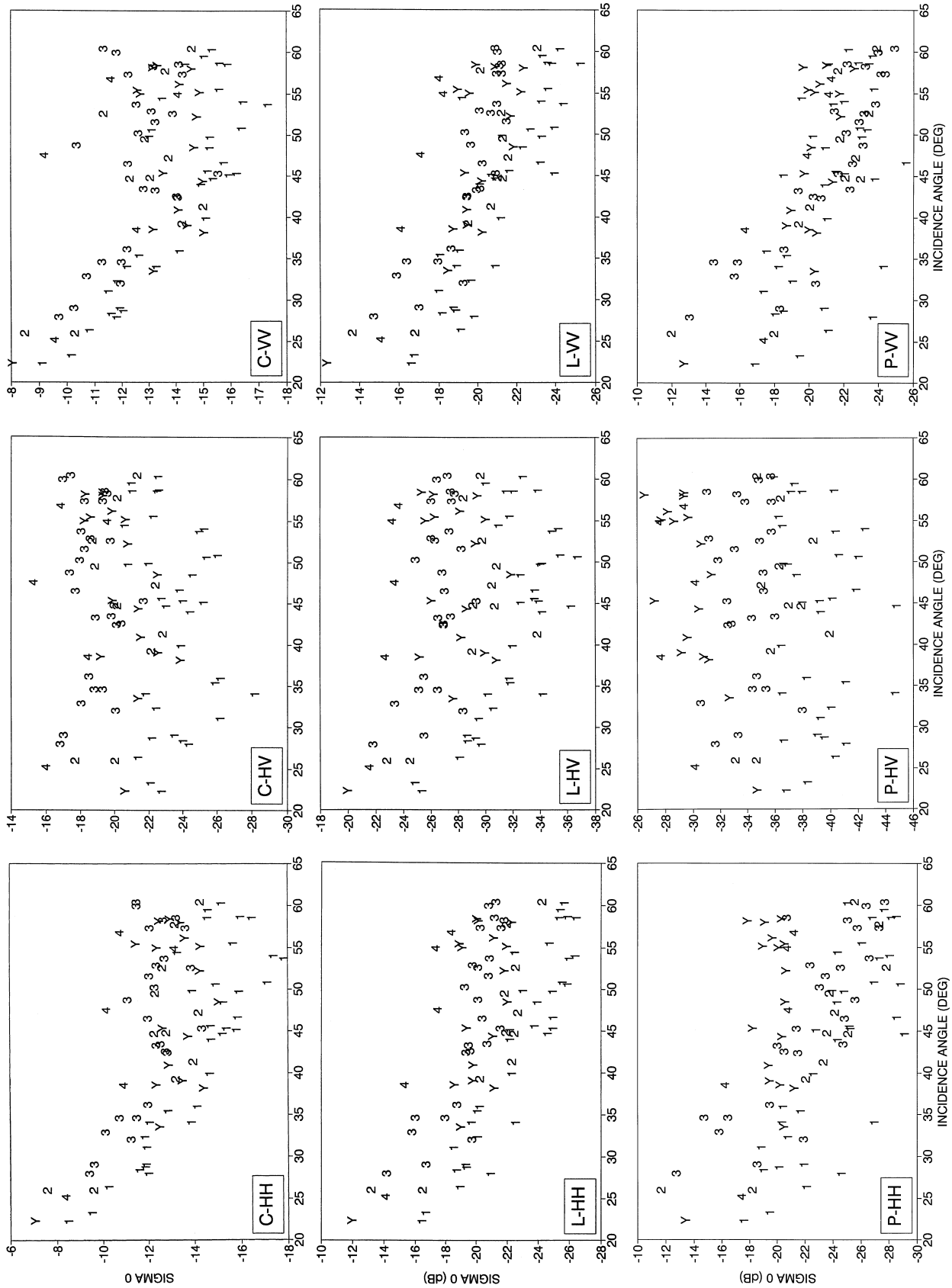

Figure 5. Backscattering coefficients (σ^0) of field sites in relation to incidence angle, at C-, L-, and P-bands and at HH, HV, and VV polarizations. Woody shrub density classes 1–4 and yucca class (Y) same as given in Figures 2–3 and Table 1.

erately dense stand gave densities of 367 ha^{-1} for individuals, many of which were multistemmed, and 1000 ha^{-1} for leaf rosettes. Understory vegetation of sites in Class Y varied widely, from grassland to dense shrubs.

Changes in shrub and yucca density in the 3 years from the 1990 overflight to the 1993 ground truth observations were assumed to be slight. This assumption is based on 15 years of field experience in the area by the senior author, including repeated quantitative measurement of vegetation (Musick, in press). In addition, several sites previously sampled and photographed in 1981–1982 (Warren and Hutchinson, 1984) were revisited in 1993 and found to have changed little in shrub and yucca density.

Differences in the amount of herbaceous vegetation were not considered in the classification because the density and moisture content of herbaceous foliage vary so strongly in response to seasonal moisture that observations 3 years after the overflight would be unreliable as ground truth. The density and species composition of herbaceous vegetation varied widely among sites at the lower shrub densities (Classes 1 and 2). Class 1 included sites ranging from bare ground to the densest grassland sites in the area, which were in swales and playas that receive extra moisture from runoff (see Fig. 3).

AIRSAR Data Calibration and Processing

The multifrequency and fully polarimetric SAR data used in this study were processed at the Jet Propulsion Laboratory (JPL) using SAR processor version 2.40. Four 6-ft (2 m) high aluminum corner reflectors provided by JPL were deployed with an inclination angle of 10° on a smooth (radar dark) playa surface within the Jornada site (see CR on Fig. 2). These reflectors were imaged during two of the three flightlines. The reflector responses were analyzed by one of the authors (ggs) using MacSigma0 calibration software provided by JPL (Norikane and Freeman, 1993). Calibration correction factors for radar backscatter and phase angles for all three SAR frequencies were computed using the corner reflector analysis software available as part of MacSigma0. Backscattering coefficient (σ^0) values for each of the 59 sites mentioned above were computed for each SAR frequency and polarization after applying the correction factors derived using the corner reflectors.

Of the 59 sites, 31 were imaged on two AIRSAR flightlines at different incidence angles, and one site was imaged on all three flightlines. Sites were imaged at radar incidence angles ranging from 22° to 60° from nadir.

RESULTS

Backscatter Variation with Incidence Angle

Backscattering coefficients and other measures of the polarization response for a given site may vary considerably with incidence angle, and some means of eliminating or minimizing the effects of variation in incidence angle is necessary when radar signatures of different sites are compared. In many studies, comparisons among sites are limited to sites within a narrow range of incidence angles (e.g., Dobson et al., 1992). This approach was not feasible for the present study because the distribution of vegetation types over the landscape and problems in accurately locating and delineating sites on the imagery prohibited selection of several sites of each type at a given incidence angle.

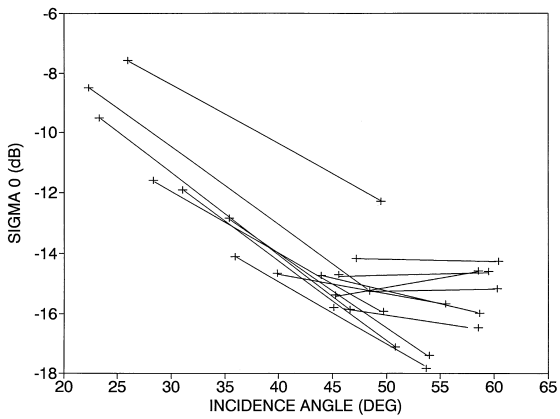

Figure 6. Change in cross-polarized C-band backscattering coefficient (σ^0HV) with incidence angle, for sites in shrub density classes 1 and 2 imaged at more than one angle. Lines connect points for same site.

The approach taken in the present study was to examine plots of variation in radar signature with incidence angle and select a range of angles which had mimimal variation in signature but was broad enough to contain several sites of each vegetation class. Two kinds of plots were examined for each quantitative measure of radar signature. In the first, data points identified by vegetation class were plotted for each site at each of the one to three incidence angles at which data for the site were obtained (Fig. 5). In the second type of plot, only the data for sites viewed at more than one incidence angle were used; data points were identified by site number, and the two or three data points per site were connected using straight lines to aid in identifying an angular range with little change in signature. For ease of visual interpretation, separate plots were made for each group of similar vegetation classes (1–4 and Y). Plots of this type were too numerous to present in their entirety; an example is shown in Figure 6.

Effects of incidence angle on single-channel σ^0 values were examined by means of the plots previously described (i.e., Fig. 5 and all plots of type shown in Fig. 6). Copolarized backscatter exhibited a stronger dependence on incidence angle than did crosspolarized backscatter, in agreement with previous studies (e.g., Fung and Ulaby, 1983). Inspection of these plots indicated that the inci-

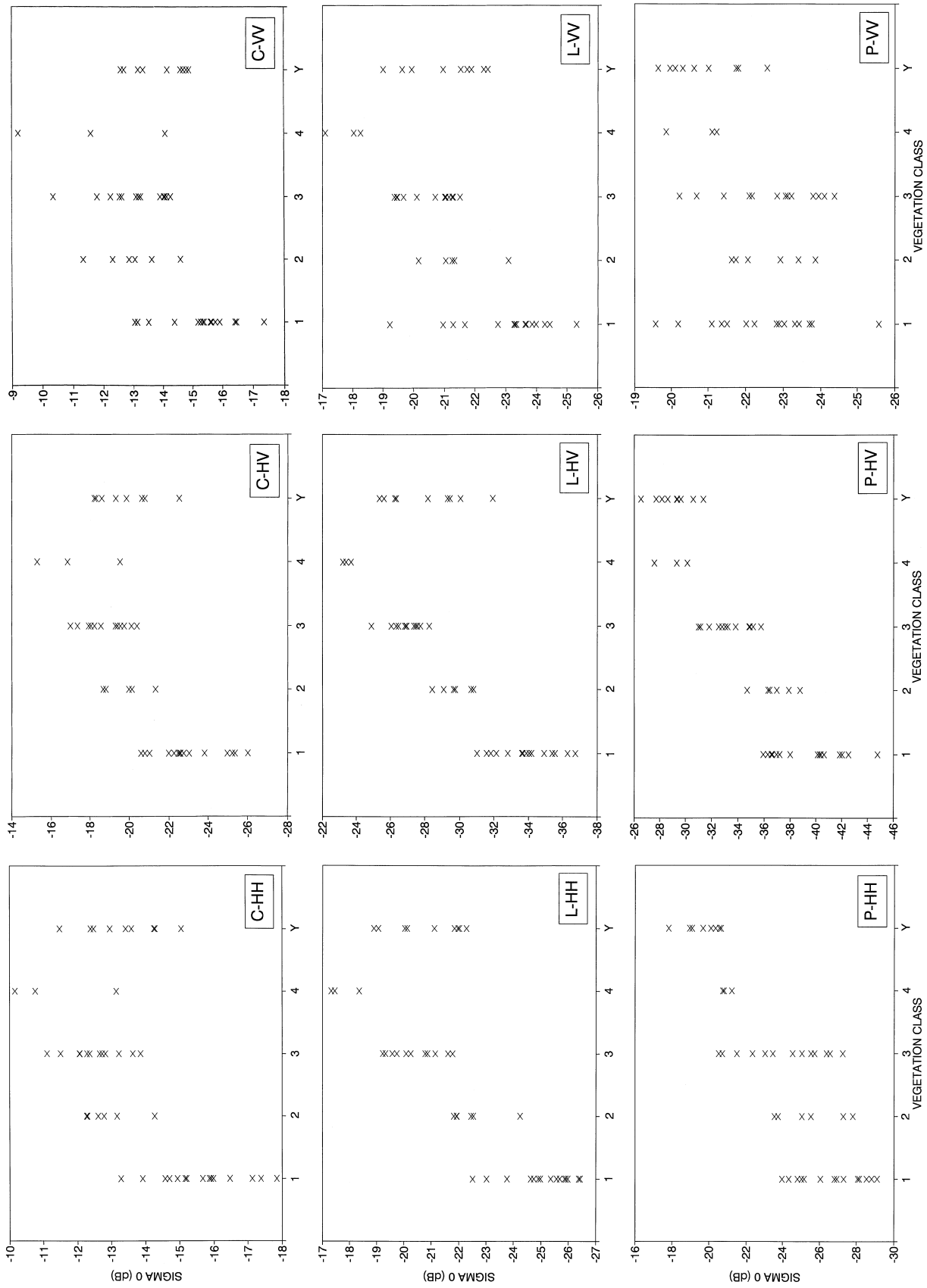

Figure 7. Backscattering coefficients (σ^0) of field sites at C-, L-, and P-bands, and at HH, HV, and VV polarizations in relation to vegetation class. Woody shrub density classes 1–4 and yucca class (Y) same as given in Figures 2–3 and Table 1. Data are restricted to incidence angles $>42°$ and to maximum angle if site was imaged at more than one angle $>42°$.

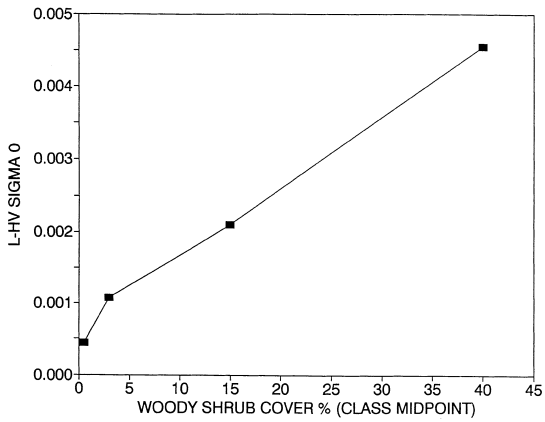

Figure 8. Mean L-band σ^0HV (in natural units) of woody shrub density classes in relation to midpoint of class shrub cover percentage limits, as given in Table 1.

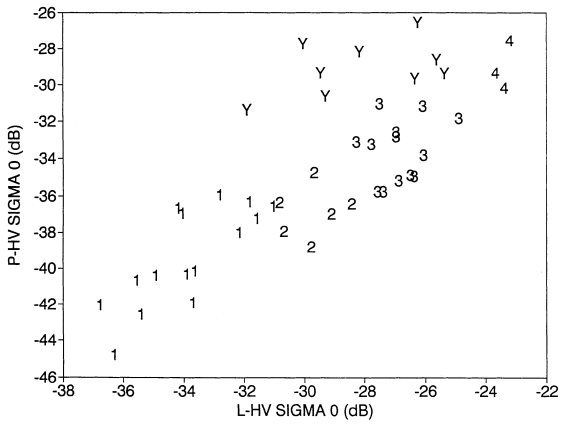

Figure 9. P-band σ^0HV in relation to L-band σ^0HV for field sites. Data are restricted to incidence angles >42° and to maximum angle if site was imaged at more than one angle >42°. Vegetation class symbols as in Table 1.

dence angle range from 42° to 60° provided the best compromise between minimizing the effects of variation in incidence angle on σ^0 and maximizing the number of sites for all vegetation classes. The plots indicated that effects on σ^0 of this range of incidence angle variation would be ±1.5 dB or less for most sites. Forty-six of the 59 sites were imaged at least once within the selected incidence angle range. For sites viewed at more than one angle within this range, the σ^0 value obtained at the greatest incidence angle was used for subsequent analysis.

Backscatter Response to Shrub and Yucca Density

Backscattering coefficients tended to increase with woody shrub density (Classes 1–4) in most wavebands and polarization modes (Fig. 7). There was substantial overlap among shrub density classes in most cases, but separability of classes was greatest for L-HV. Lack of overlap between Classes 1 and 2 in L-HV σ^0 indicates a surprising capacity to detect small amounts of shrub cover (1–5% for Class 2, compared to <1% for Class 1).

Because shrub cover at the field sites was specified only in terms of broad density classes (Table 1), the form of the relation between L-HV σ^0 and shrub density cannot be determined with great precision. However, a plot of class means of σ^0 against the midpoint shrub density of each class suggests that the increase in backscatter with shrub density is linear, or nearly so, when σ^0 is expressed in natural units (Fig. 8).

Sites with dense yucca (Class Y) tended to have moderate to high backscattering coefficients in all waveband-polarization mode combinations, with P-HH yielding the least overlap of this class with the others (Fig. 7). Because no single channel was capable of complete separation of this class, two-channel combinations were examined. The most effective combination was found to be P-HV with L-HV, in which the yucca sites were distinguishable by their higher P-HV backscatter than other sites with similar L-HV backscatter (Fig. 9).

DISCUSSION

Crosspolarized backscatter was generally more effective than copolarized backscatter in distinguishing vegetation classes. Crosspolarized backscatter is very sensitive to multiple scattering by vegetation canopy elements, whereas copolarized backscatter also includes strong contributions from the underlying surface (Fung and Ulaby, 1983; Evans et al., 1986; Ferrazzoli and Guerriero, 1995). It is also possible that data dispersion due to variation in incidence angle was not completely removed from the copolarized data by our restricting the incidence angle range to 42–60°.

Wavebands differ in the optimum dimensions of canopy scattering elements (i.e., stems and leaves or leaflets) for maximum backscatter. Observations of radar backscatter from forests indicate that C-band is most sensitive to leaves and small branches, L-band to branches of intermediate size, and P-band to trunks and the largest branches (Dobson et al., 1992; Ferrazzoli et al., 1992; Le Toan et al., 1992; Moghaddam and Saatchi, 1995; Kasischke et al., 1995). Modeling of volume scattering by canopies of randomly oriented cylinders indicates that backscattering in C-, L-, and P-bands is optimally sensitive to cylinder diameters of <0.8 cm, 1–3 cm, and 3–6+ cm, respectively; as diameter decreases below the optimum for each band, elements are increasingly transparent to that band (Ferrazzoli and Guerriero, 1995).

These differences in optimum canopy element size for maximum backscatter are likely responsible for waveband differences in the ability to distinguish shrub density classes and yucca sites. Leaves and stems of the herbaceous vegetation in this study area are generally <1 cm

in diameter and would therefore have been transparent or nearly so to L- and P-bands. The woody shrub canopies contain many stems of intermediate size (1–3 cm) and would therefore be expected to contribute strongly to L-band backscatter. Woody shrubs sometimes have larger stems that are near the optimal size for P-band backscatter, but the abundance of these larger stems depends strongly on the size of the individual shrubs and is not necessarily correlated with total shrub cover at a site. Stems of intermediate size are more universally present in mature shrubs, which would explain why L-band backscatter provides a better estimate of shrub cover than P-band. Yuccas have large stems (10 cm) which would be strong backscatterers in P-band, but lack stems of intermediate size. Stands of dense yucca would therefore tend to have high P-band backscatter relative to L-band.

The major influences on cross-polarized backscattering for a given band and site would therefore appear to be 1) the density of the different growth forms (i.e., herbaceous plants, woody shrubs and yucca) at the site, 2) the size distribution of the canopy structural elements, which varied with growth form, and 3) dependence of volume scattering on the size of the canopy structural elements relative to the radar wavelength (Ferrazzoli and Guerriero, 1995).

The two major concerns regarding the generality of the results are the atypically high soil moisture levels and the lack of gravelly or rocky soils in the study area. The moist soil may have enhanced canopy volume backscattering, and thus the effects of differences in canopy structure, by increasing the radiation backscattered via the ground-to-canopy pathway. If gravelly and rocky soils were included, greater variation in soil surface backscattering might obscure the effects of canopy structural differences. Further studies of grassland–shrubland transition zones should be conducted under the more typical conditions of dry soil and with gravelly and rocky soils included. Also, application of backscattering models specifically devised for discontinous canopies (Sun et al., 1992; Wang et al., 1993; Sun and Ranson, 1995) would be useful in identifying the major sources of backscattered radiation under different soil moisture conditions.

CONCLUSIONS

In mixtures of varying amounts of woody shrubs and herbaceous plants, L-band σ^0HV provided the best separability of shrub density classes and appeared to be capable of detecting small amounts of woody shrub cover. The sensitivity of L-band backscattering to the amount of woody shrub cover could be accounted for differences in stem size between shrub and herbaceous canopies. Shrub canopies contain a large proportion of medium-sized stems to which L-band is optimally responsive, whereas stems of this size are mostly lacking in herbaceous plants and yucca.

The relation of P- to L-band σ^0HV was the most effective means of identifying sites with dense yucca. The enhanced backscattering in P-band relative to L-band of dense yucca stands may be explained by the unusual structure of yucca canopies, which have large stems optimal for P-band backscatter while lacking medium-sized stems.

Further study would be necessary to determine whether the relation of radar backscatter to shrub density observed in this study would also be observed when the soil was dry and when gravelly and rocky soils were included.

The NASA/JPL AIRSAR is presently the only multifrequency and fully polarimetric SAR instrument available for research that can acquire the high resolution L-HV and P-HV data shown here to be optimal for discriminating herbaceous vegetation and woody shrubs at the Jornada study site. Future spaceborne SAR sensors that could be useful in similar studies include: 1) Radarsat II, which will provide both copolarized and cross-polarized C-SAR data, and 2) LightSAR, a polarimetric L-band SAR (1.2 GHz) that is currently in the development stage at the Jet Propulsion Laboratory. Unfortunately, neither of these sensors will have P-band capability.

We thank R. P. Gibbens for assistance in site selection and information on site history, Marlene Tuesink for her support during field work and in setting up the corner reflectors, and David "John" Chadwick for laboratory determinations of soil moisture content. This research was made possible by SIR-C funding to G. Schaber from NASA/JPL to the U. S. Geological Survey (Contract WO8864) and to Northern Arizona University (Contract 960529).

REFERENCES

Blom, R., and Elachi, C. (1981), Spaceborne and airborne imaging radar observations of sand dunes. *J. Geophys. Res.* 86:3061–3073.

Breed, C. S., and Reheis, M., Eds. (in press), *The Desert Winds Project: Monitoring Wind-Related Surface Processes in Arizona and New Mexico*, USGS Professional Paper 1598, U.S. Geological Survey, Washington, DC.

Buffington, L. C., and Herbel, C. H. (1965), Vegetational changes on a semidesert grassland range from 1858 to 1963. *Ecol. Monogr.* 35:139–164.

Dobson, M. C., Ulaby, F. T., LeToan, T., Beaudoin, A., Kasischke, E. S., and Christensen, N. (1992), Dependence of radar backscatter on coniferous forest biomass. *IEEE Trans. Geosci. Remote Sens.* 30:412–415.

Evans, D. L., Farr, T. G., Ford, J. P., Thompson, T. W., and Werner, C. L. (1986), Multipolarization radar images for geologic mapping and vegetation discrimination. *IEEE Trans. Geosci. Remote Sens.* GE-24:246–257.

Evans, D. L., Farr, T. G., van Zyl, J. J., and Zebker, H. A. (1988), Radar polarimetry: analysis tools and applications. *IEEE Trans. Geosci. Remote Sens.* 26:774–789.

Ferrazzoli, P., and Guerriero, L. (1995), Radar sensitivity to tree geometry and woody volume: a model analysis. *IEEE Trans. Geosci. Remote Sens.* 33:360–371.

Ferrazzoli, P., Paloscia, S., Pampaloni, P., Schiavon, G., Solimini, D., and Coppo, P. (1992), Sensitivity of microwave measurements to vegetation biomass and soil moisture content: a case study. *IEEE Trans. Geosci. Remote Sens.* 30: 750–756.

Fung, A. K., and Ulaby, F. T. (1983), Matter-energy interaction in the microwave region. In *Manual of Remote Sensing*, 2nd ed. (R. N. Colwell, Ed.), American Society of Photogrammetry, Falls Church, VA, pp. 115–164.

Greeley, R., and Blumberg, D. G. (1995), Preliminary analysis of Shuttle Radar Laboratory (SRL-1) data to study aeolian features and processes. *IEEE Trans. Geosci. Remote Sens.* 33:927–932.

Greeley, R., Christensen, P., and Carrasco, R. (1989), Shuttle radar images of wind streaks in the Altiplano, Brazil. *Geology* 17:665–668.

Grover, H. D., and Musick, H. B. (1990), Shrubland encroachment in southern New Mexico, U.S.A.: an analysis of desertification processes in the American southwest. *Clim. Change* 17:305–330.

Kasischke, E. S., Christensen, N. L., Jr., and Bourgeau-Chavez, L. L. (1995), Correlating radar backscatter with components of biomass in loblolly pine forests. *IEEE Trans. Geosci. Remote Sens.* 33:643–659.

Lancaster, N., Gaddis, L., and Greeley, R. (1992), New airborne imaging radar observations of sand dunes: Kelso Dunes, California. *Remote Sens. Environ.* 39:233–238.

Le Toan, T., Beaudoin, A., Riom, J., and Guyon, D. (1992), Relating forest biomass to SAR data. *IEEE Trans. Geosci. Remote Sens.* 30:403–411.

Martin, W. C., and Hutchins, C. R. (1980), *A Flora of New Mexico*, A. R. Gantner Verlag K. G., Vaduz, Germany.

Moghaddam, M., and Saatchi, S. (1995), Analysis of scattering mechanisms in SAR imagery over boreal forest: results from BOREAS '93. *IEEE Trans. Geosci. Remote Sens.* 33:1290–1296.

Musick, H. B. (in press), Field monitoring of vegetation characteristics related to surface changes in the Yuma Desert, Arizona and at the Jornada Experimental Range in the Chihuahuan Desert, New Mexico. In *The Desert Winds Project: Monitoring Wind-Related Surface Processes in Arizona and New Mexico* (C. S. Breed and M. Reheis, Eds.), USGS Professional Paper 1598, U.S. Geological Survey, Washington, DC.

Norikane, L., and Freeman, A., 1993, *User's Guide to MacSigma0*, JPL Document D-10599, Jet Propulsion Laboratory, Pasadena, CA, 147 pp.

Pieper, R. D., and McDaniel, K. C. (1989), Ecology and management of broom snakeweed. In *Snakeweed: Problems and Perspectives*, New Mexico Agricultural Experiment Station Bulletin 751, pp. 1–12. Las Cruces, NM.

Schlesinger, W. H., Reynolds, J. F., Cunningham, G. L., et al. (1990), Biological feedbacks in global desertification. *Science* 247:1043–1048.

Sun, G., and Ranson, K. J. (1995), A three-dimensional radar backscatter model of forest canopies. *IEEE Trans. Geosci. Remote Sens.* 33:372–382.

Sun, G., Simonett, D. S., and Strahler, A. H. (1992), A radar backscatter model for discontinuous coniferous forests. *IEEE Trans. Geosci. Remote Sens.* 29:639–650.

Wang, Y., Day, J., and Sun, G. (1993), Santa Barbara microwave backscattering model for woodlands. *Int. J. Remote Sens.* 14:1477–1493.

Warren, P. L., and Hutchinson, C. F. (1984), Indicators of rangeland change and their potential for remote sensing. *J. Arid Environ.* 7:107–126.